Selective deposition of Ta2O5 by adding plasma etching super-cycles in plasma enhanced atomic layer deposition steps

Rémi Vallat, Rémy Gassilloud, Brice Eychenne, Christophe Vallée

Selective deposition of Ta_2O_5 by adding plasma etching super-cycles in plasma enhanced atomic layer deposition steps

Rémi Vallat
Univ. Grenoble Alpes, LTM-CNRS, F-38000 Grenoble, France and CEA, LETI, Minatec Campus, F-38054 Grenoble, France

Rémy Gassilloud
CEA, LETI, Minatec Campus, F-38054 Grenoble, France

Brice Eychenne and Christophe Vallée[a)]
Univ. Grenoble Alpes, LTM-CNRS, F-38000 Grenoble, France

(Received 19 July 2016; accepted 10 October 2016; published 25 October 2016)

In this paper, a new route for a selective deposition of thin oxide by atomic layer deposition is discussed. The proposed process is using super cycles made of an additional plasma etching step in a standard plasma enhanced atomic layer deposition (PEALD) process. This allows the selective growth of a thin oxide on a metal substrate without a specific surface deactivation by means of self assembled monolayer. It is shown that adding a small amount of NF_3 etching gas to an oxygen plasma gas every eight cycles of the PEALD process helps to fully remove the Ta_2O_5 layer on Si and/or SiO_2 surface while keeping few nanometers of Ta_2O_5 on the TiN substrate. NF_3 addition is also used to increase the incubation time before Ta_2O_5 growth on Si or SiO_2 substrate. In this way, a selective deposition of Ta_2O_5 on the TiN substrate is obtained with properties (density, leakage current…) similar to the ones obtained in a conventional PEALD mode. Hence, the authors demonstrate that a future for selective deposition could be a process using both PEALD and atomic layer etching. © *2016 American Vacuum Society*. [http://dx.doi.org/10.1116/1.4965966]

I. INTRODUCTION

At advanced nodes, lithography starts to dominate the wafer cost [extreme ultraviolet (EUV), managing multiple mask passes (per layer) and pattern placement error…]. Therefore, complementary techniques are needed to continue 2D scaling and extend the Moore's law.[1] Selective deposition, a bottom/up technique, is one of them because it can be used to increase and enhance patterning capabilities at a very low cost. Of all the different deposition processes, atomic layer deposition (ALD) is the more suitable tool for developing a selective process due to its high surface sensitivity. Hence, ALD may allow to overcome lithography limits, being currently used for self-aligned double and quadruple patterning.[2–5]

The strong sensitivity of ALD to the chemistry of the substrate has been the source of the development of a new process named selective-area (or area-selective) ALD.[6–11] The growth with this method is allowed or inhibited on a selective area by using a specific passivation or protection of the surface in order to limit its chemical reaction with the ALD precursor. This surface deactivation is usually obtained by using organic groups such as self-assembled monolayers (SAM). The idea is to chemically and locally bond a molecule directly to the surface in order to inhibit reactive sites and then prevent further reactions between the precursor molecules and the surface. Alkyl silanes with long hydrocarbon chains terminated with a reactive silane end groups are well known to inhibit the chemical reactions by modifying the hydrophilic surface (-OH terminated, for example) to a hydrophobic surface. SAM of octadecyltrichlorosilane as surface modifying agents for area selective ALD have been widely investigated for the growth of oxides (HfO_2, TiO_2, ZrO_2, Al_2O_3, and ZnO)[6–8,12–16] and metals (Ru, Pt, and Ir)[10,11,17–20] on 2D or 3D features.[21] SAM are formed by immersing the substrate into a solution containing the SAM-forming precursor molecules or by using a vapor phase process.[19] Some limiting steps for this method are: (1) the SAM must be defect-free, which (2) requires extended SAM deposition times.[6] Therefore, some authors have proposed to use lithographically defined polymer films instead of SAM (Refs. 14 and 22) or to transfer a block copolymer mask.[23] The process has also been improved using both selective ALD and selective removal of the SAM (Refs. 13 and 24) or by using patterned surfaces[25,26] and vacuum UV light.[27]

Another pathway for selective area deposition with ALD is to take advantage of the inherent substrate-dependent growth initiation by using different precursors or "water-free" processes.[14,28,29] Atanasov *et al.*[28] have obtained up to 2 nm of selective ALD growth of TiO_2. This method based on nucleation delay between two surfaces has the advantage to avoid the use of complex organic blocking layer. But it is limited to the initial nucleation delay of ALD for two different substrates as illustrated in Fig. 1.

In this work, we propose a new pathway, based on nucleation delay and on the joint use of a plasma enhanced atomic layer deposition (PEALD) mode and a plasma etching mode, such as atomic layer etching (ALE), by adding a chemical plasma etching step to the ALD ones. This process has the advantage of being simple, easy to integrate, and with no use of SAM, as illustrated in Fig. 2. The thin oxide film is deposited in the PEALD mode. An oxygen plasma is used to

a)Electronic mail: christophe.vallee@cea.fr

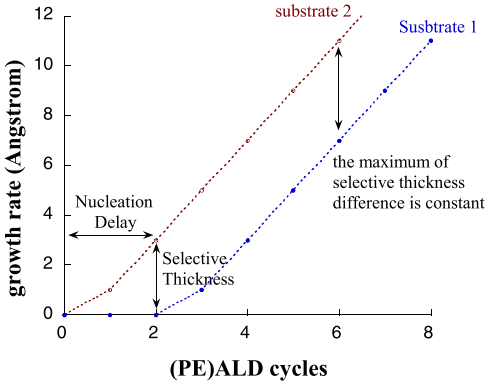

FIG. 1. (Color online) Illustration of a selective deposition process only based on the nucleation delay induced by the ALD process.

oxidize the ligands of the precursor. The different nucleation delay observed either on metal, oxide, or silicon substrate will allow to start with a few nanometers of selective deposition. After several cycles, an etching gas is added to the oxygen plasma in order to remove the oxide from the surface with the longer nucleation delay. The etching gas composition is chosen in order to passivate the surface after all the oxide has been etched, subsequently creating a new nucleation delay which is longer than the previous one. Then, a new PEALD mode is started, and after several cycles, the plasma etching mode is used again. This PEALD + ALE super cycle can be repeated several times, depending on the thickness target for the oxide. In this paper, we will use this new process for the selective area deposition of Ta_2O_5 as example, but it seems not restricted to this oxide.

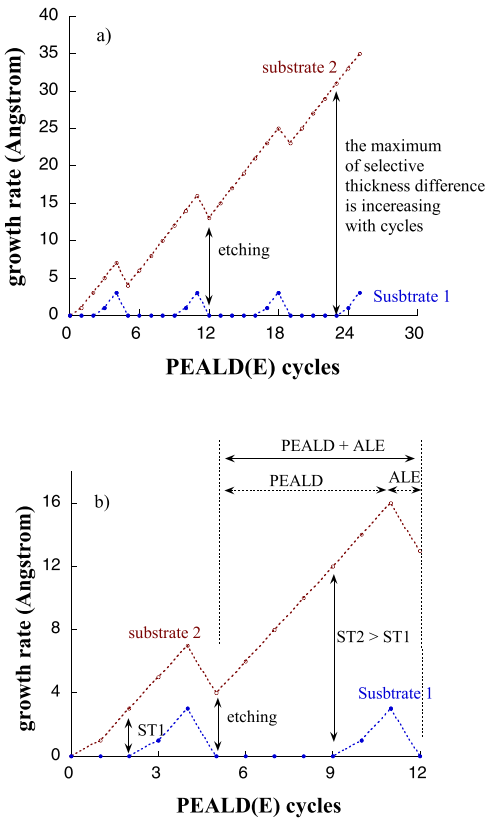

FIG. 2. (Color online) Illustration of a selective deposition process based on the combination of PEALD and ALE processes. (a) shows that the selective thickness is increasing with time (no limits). (b) is a zoomed-in view of (a) for a better understanding of the process (ST = selective thickness).

II. EXPERIMENT

A. PEALD reactor and Ta_2O_5 deposition

The selective depositions were made in a tool equipped with a pulsed liquid injection system for precursor distribution and a dual frequency plasma assistance[30] on 200 and 300 mm wafers. This versatile tool allows the deposition of oxides, metals nitrides in CVD, PECVD, ALD, or PEALD modes.[30–32] Tertiary-butylimidotrisdiethyl-amino tantalum (TBTDET) liquid precursor was used in combination with an O_2 plasma for the PEALD of Ta_2O_5 oxide. The O_2 gas was also used for the purge as first proposed by Choi *et al.*[33] For the etching step, NF_3 gas was added to O_2 (See Secs. III B and III C). The deposition module consists of an evaporating furnace and a deposition chamber. The furnace is used for the liquid precursor flash vaporization. The liquid precursor is carried using He to the evaporating furnace where it is introduced, thanks to a liquid injector. The vaporized precursor is then introduced into the deposition chamber through a showerhead with two separated paths: one for the precursor gas and the other for the reactant gas. The deposition chamber is a capacitively coupled plasma chamber with a distance of a few centimeters between the showerhead and the substrate holder. Two independently controlled generators can be used to power the plasma at 13.56 MHz and/or 350 kHz. Both generators deliver the power at the showerhead, the substrate holder being grounded. For this paper, only the plasma in the 13.56 MHz mode has been used either for oxidation in PEALD process ($Ar + O_2$ plasma) or etching ($Ar + O_2 + NF_3$).

B. Characterization tools

Thickness, density, and roughness were measured by x-ray reflection (XRR), using a Jordan Valley JVX5200 for process development (deposition and etching) and using a Panalytical X'Per Pro tool for selective deposition tests (samples on holder). Chemical composition was measured with x-ray photoelectron spectroscopy (XPS) using a Thermo Scientific Theta 300, with Al-Kα, 400 μm and 100 eV beam. Electrical characterizations in the DC mode were performed in air using a Keithley 2635a Source Meter unit, with the bottom electrode grounded.

III. RESULTS AND DISCUSSION

A. PEALD of Ta_2O_5

The TBTDET precursor and O_2 reactive gas are pulsed separately into the deposition chamber. The TBDET pulse duration is 4 s, and the O_2 plasma pulse duration is 2 s with a RF power of 75 W. The O_2 gas is highly diluted, by a ratio of 1:10, in Ar gas (250 sccm of O_2 and 2500 sccm of Ar) in order to set the working pressure at 2 Torr.

First of all, the ALD window of the thermal Ta_2O_5 ALD process has been determined (plateau of the thickness as a function of deposition temperature). For this purpose, depositions have been performed at 5 different temperatures (250, 300, 350, 375, and 400 °C) with 11 ALD cycles on the Si substrate. Thicknesses are then obtained, thanks to XRR measurements and plotted as a function of deposition temperature, as illustrated in Fig. 3. The ALD plateau (deposition limited by surface reactions) corresponds to a deposition temperature lower than 350 °C. After 350 °C, the oxide thickness increases strongly with the temperature and thus switching from and ALD mode to a CVD mode for which the deposition is directly linked to the temperature. Therefore, in the following, the deposition temperature has been fixed to 325 °C for all the PEALD and selective depositions.

In a second time, we have studied the growth per cycle and nucleation delay for PEALD of Ta_2O_5 as a function of the substrate material. For this purpose, three different substrates have been used: Si with native oxide, SiO_2 (thermal oxide 100 nm), and TiN 10 nm. The number and the nature of nucleation sites will differ for the three substrates, possibly leading to different nucleation delays, consequently yielding a "first" selective thickness that may be useful for our selective process [ST1 in Fig. 2(b)]. For all three substrates, the growth per cycle and nucleation delay have been quantified using XRR measurements by evaluating the thickness of the film deposited by PEALD after 11 cycles, 21 cycles, 31 cycles, 41 cycles, and 51 cycles.

The resulting measured thicknesses are reported in Fig. 4. It shows that Si and SiO_2 substrates have equivalent nucleation delay while the Ta_2O_5 deposited on TiN has a shorter incubation time. The selective thickness for growth on TiN versus Si or SiO_2 is equal to 1.5 nm. After 11 cycles, the growth per cycle is about 0.95 Å/cycle and is more or less the same whatever be the substrates used since Ta_2O_5 is now deposited on top of Ta_2O_5 independently from the substrates.

Using the XRR measurements, we also obtained the density and roughness of the layers deposited on each of the three substrates. The measured density of the oxide on the three substrates is between 8.1 and 8.3 g/cm^3, which is close to the theoretical value of 8.5 g/cm^3, thus showing no influence of the substrate. Identically to the density, the roughness is not influenced by the substrate, yielding relatively smooth films with a roughness about 3 Å. A mapping of the

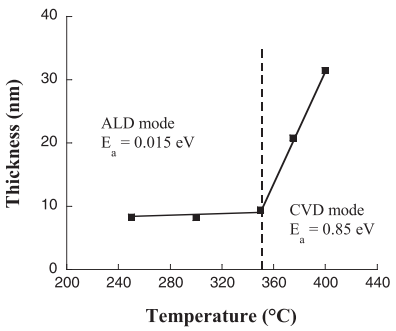

FIG. 3. Ta_2O_5 film thickness measured by XRR vs substrate temperature.

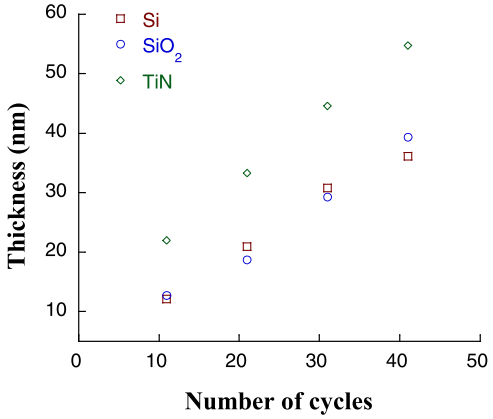

FIG. 4. (Color online) Ta_2O_5 film thickness measured by XRR vs number of PEALD cycles for three different substrates: Si, SiO_2, and TiN.

300 mm wafers by ellipsometry has shown a very good uniformity with a maximum 5% thickness standard deviation.

B. Plasma etching of Ta_2O_5

For the Ta_2O_5 etching, we used the NF_3 cleaning gas available inside the PEALD reactor. The tool is dedicated to the deposition of nitrides or oxides while the capacitive plasma configuration of the electrodes also enables to develop a plasma etch process in the chamber. Fluorine-based compounds are often used for the plasma etching of Ta, TaN, or Ta_2O_5 materials in reactive ion etching or inductively coupled plasma modes since the boiling temperature of TaF_5 is very low, about 230 °C.[34,35] We thus have evaluated the Ta_2O_5 etching rate as a function of NF_3 flow rate dilution in $O_2 + Ar$. The plasma RF power has been fixed to 75 W, and the pressure was fixed at 2 Torr. The results are given in Table I. This shows that only a very low NF_3 flow rate (<10 sccm) allows the low etch rate needed for a precise atomic etching of the oxide.

Ta_2O_5 etching selectivity over SiO_2 or Si is known to be on the order of 5–10 depending on the plasma chemistry.[35] We have also tested the influence of NF_3 addition on SiO_2 etching. The results are given in Table II. From the value obtained with 5 sccm of NF_3, we found that a Ta_2O_5/SiO_2 selectivity of 1/4. Therefore, one can hope to etch Ta_2O_5 on a Si or SiO_2 surface with limited damages to the substrate.

From all these results, we decided to use the following gas mixture for the selective deposition process etching step (see the next section): NF_3 (5 sccm) + O_2 (250 sccm) + Ar (2500 sccm).

C. Selective deposition of Ta_2O_5

The selective deposition process is summarized in Fig. 5. As already said, the O_2 flow is never stopped during the

TABLE I. Etch rate of Ta_2O_5 vs NF_3 flow rate in the plasma chamber.

NF_3 flow rate (sccm)	125	50	5
O_2 flow rate (sccm)	250	250	250
Ta_2O_5 etch rate (nm/s)	≫2	2	0.025

TABLE II. Etch rate of SiO_2 vs $NF_3 + O_2$ flow rates in the plasma chamber.

NF_3 flow rate (sccm)	10	10	5
O_2 flow rate (sccm)	0	250	250
SiO_2 etch rate (nm/s)	0.33	0.22	0.1

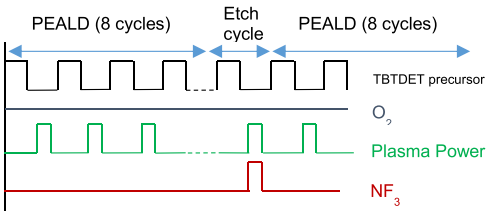

FIG. 5. (Color online) illustration of the selective deposition process. A super-cycle corresponds to eight PEALD cycles + one etch cycle.

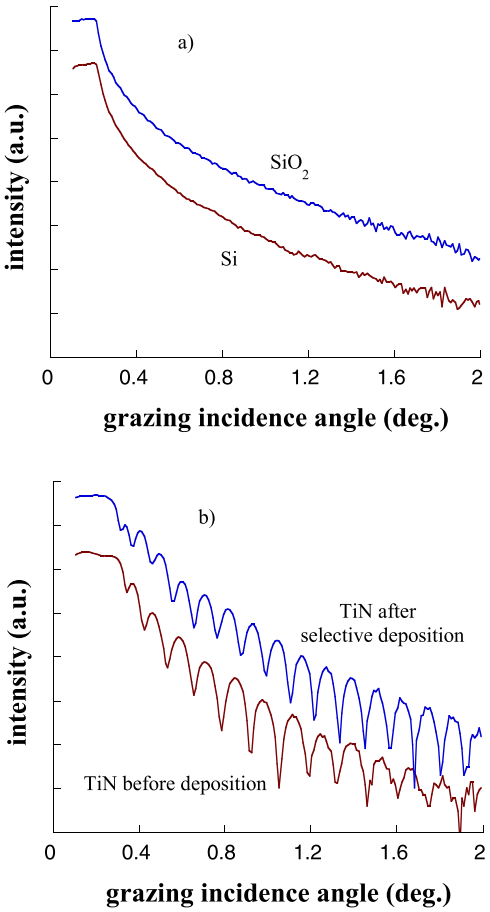

FIG. 6. (Color online) Top (a): XRR graphs recorded after Ta_2O_5 deposited on Si and SiO_2 substrates with the selective deposition process. Bottom (b): XRR graphs recorded before and after Ta_2O_5 selectively deposited on the TiN substrate.

TABLE III. Ta_2O_5 film thickness and density obtained from XRR measurements on Si, SiO_2, and TiN substrates after the selective deposition process.

Number of super cycles	Ta_2O_5 thickness on Si/SiO_2 (nm)	Ta_2O_5 thickness on TiN (nm)	Ta_2O_5 density ($g\,cm^{-3}$)
11	0/0	3.6	6.4
22	0/0	7.1	6.1

process, and it is used for plasma oxidation as well as purge steps of the PEALD cycle. Every eight cycles a low amount of NF_3 (5 sccm) is added to O_2 gas for the etching step. This "super cycle" (PEALD + etching) can be repeated several times, depending on the desired selective thickness. In order to test and validate the process, a deposition has been carried out on the same three different substrates, i.e., Si, SiO_2, and TiN.

Figure 6 shows the XRR spectra of the three different substrates after 11 super-cycles. As can be seen in this figure, no Ta_2O_5 films are detected on Si and SiO_2 substrates while a thin film has been deposited on top of the TiN substrate. A modeling of the structure allows to extract the respective thickness and density for the Ta_2O_5 film deposited on TiN. The density of the Ta_2O_5 film deposited with the selective deposition process is lower than the nominal film by the PEALD mode with a value of about $6.4\,g\,cm^{-3}$ against $8.1\,g\,cm^{-3}$ for nominal oxide. This low value of density is not modified, even for higher thicknesses of Ta_2O_5 as reported in Table III. The growth per cycle for the selective deposition process is 0.32 Å/cycle and is about three times lower than the growth per cycle of the PEALD process.

The selective deposition on TiN has been confirmed using an angle-resolved XPS analysis performed on all the substrates after the deposition process. Figure 7 shows the O1s spectra for the Si substrate (a) and TiN substrate (b). For the TiN substrate, the O1s spectrum can be fitted with two

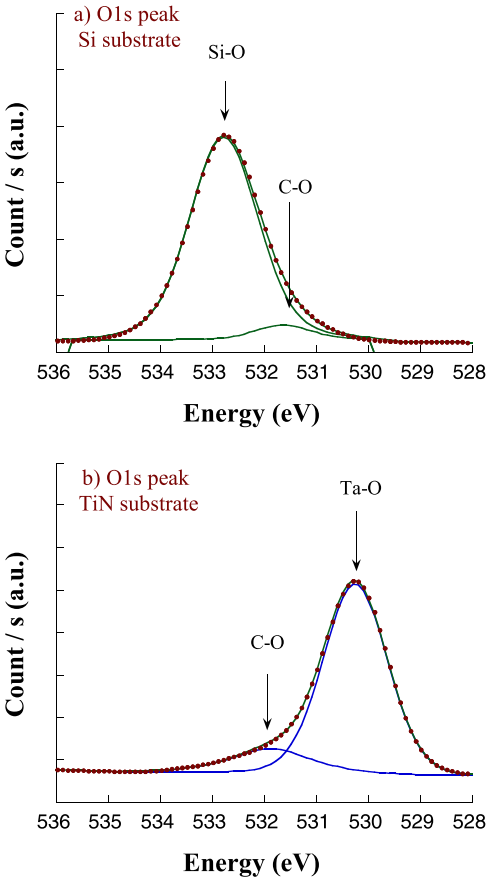

FIG. 7. (Color online) O1s photoelectron spectra recorded after the selective deposition process on (a) Si substrate and (b) TiN substrate.

Gaussian components. The first component, with a peak around 530.5 eV is attributed to O-Ta binding.[36,37] The second smaller peak at 531.7 eV is attributed to surface atmospheric contamination and O–C bonds. The O1s spectrum obtained at the surface of the Si substrate also shows two components: the first one at lower energy is due to surface contamination (O-C binding); the second peak at higher energy is attributed to O-Si binding. No components from O-Ta binding can be observed on the surface of the Si substrate, indicating a good correlation with XRR measurements in the absence of Ta_2O_5 film on the Si substrate.

The role of the NF_3 plasma in the process is not only to etch the Ta_2O_5 layer from Si or SiO_2 substrate but also to add an additional nucleation delay for Ta_2O_5 deposition on Si or SiO_2, thanks to the formation of Si–F or SiO–F bonds. We therefore compared the PEALD of Ta_2O_5 with or without pretreatment of the substrate by means of NF_3 plasma. The results of Si and TiN substrates are given in Figs. 8(a) and 8(b), respectively. These two figures show that NF_3 plasma on the Si surface increases the nucleation delay for Ta_2O_5 deposition while it has nearly no effect on TiN.

XPS analysis at varying angles have been performed on very thin Ta_2O_5 layers selectively deposited after the NF_3 surface pretreatment of the TiN and Si substrates. The two-dimensional detector integrated on the XPS tool allows to perform a parallel acquisition of the photoemission signals at six emission angles from 20° to 80° with respect to the sample normal. Figure 9 shows the intensity of the F1s XPS peak region with angles varying from high angle to low angle values. With the high angle values, only Ta_2O_5 layer is analyzed by XPS, while with low angle values, both Ta_2O_5 and the substrates are analyzed. As can be seen in Figs. 9(a) and 9(b), whatever the substrates Ta–F bonds are always detected inside the Ta_2O_5 material. The presence of Ta–F bonds inside the material after the selective deposition process is discussed below by analyzing the Ta4f peaks (Fig. 10). When decreasing the XPS incidence angle in order to probe both the Ta_2O_5 layer and the substrate, a new feature at 686.6 eV is only observed [Fig. 9(a)] for the Si substrate. This is due to the presence of Si-F bonds at the interface. After the NF_3 plasma, Si–F bonds are formed at the surface which can explain the additional delay in nucleation with NF_3 treatment observed in Fig. 8(a). No additional Ti-F bonds are observed for low values of XPS angles Fig. 9(b). To verify the absence of Ti–F bonds, we also plot in Fig. 10 the Ti2p XPS region for Ta_2O_5 deposited by PEALD (a) and by selective deposition (b). The same two contributions are observed for the two samples: Ti-O at 458.6 eV and Ti-N at 457.5 eV. No additional Ti–F bond is observed for the selectively deposited Ta_2O_5 material in Fig. 10(b). We can then assume that the TiN substrate is not modified by the NF_3 plasma that can explain identical nucleation time observed [Fig. 8(b)].

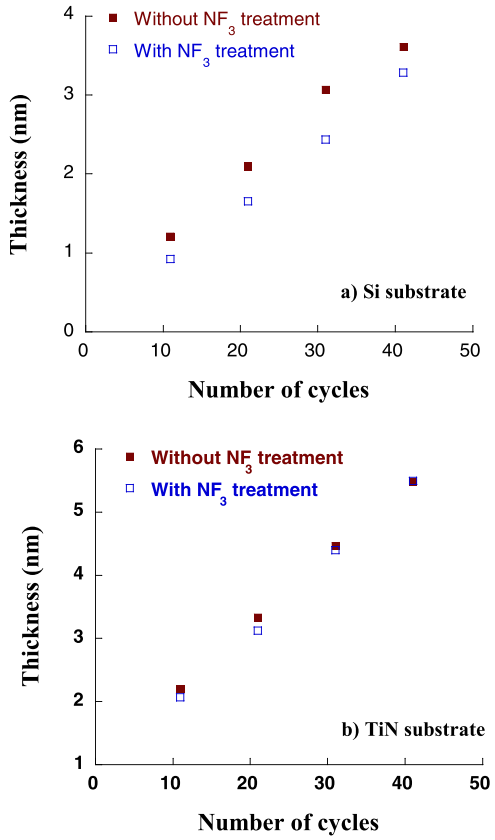

FIG. 8. (Color online) Ta_2O_5 film thickness measured by XRR vs number of PEALD cycles for untreated and NF_3 treated substrates. (a) Ta_2O_5 film thickness vs number of PEALD cycles for Si substrate exposed or not to NF_3 plasma before deposition. (b) Ta_2O_5 film thickness vs number of PEALD cycles for TiN substrate exposed or not to NF_3 plasma before deposition.

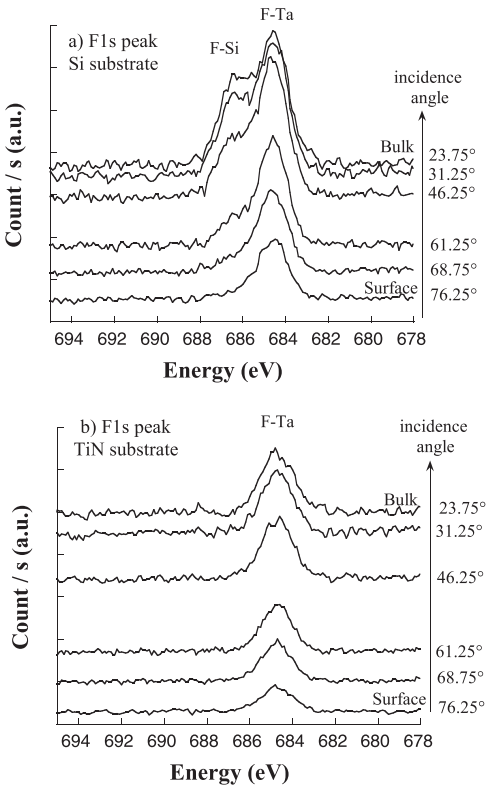

FIG. 9. XPS spectra showing the F1s region of Ta_2O_5 film recorded at different incidence angle. (a) Ta_2O_5 deposited on NF_3 treated Si substrate. (b) Ta_2O_5 deposited on NF_3 treated TiN substrate.

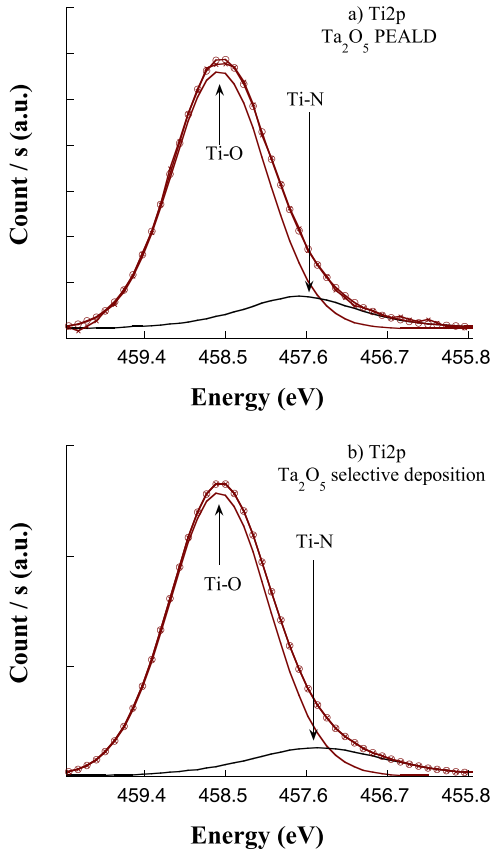

FIG. 10. (Color online) XPS spectra showing the Ti2p region of Ta_2O_5 film. (a) Ta_2O_5 deposited by PEALD. (b) Ta_2O_5 selectively deposited.

Figure 11 shows the XPS Ta4f peaks of Ta_2O_5 deposited by PEALD and with the selective deposition process on TiN substrates. The comparison between the two processes clearly evidences: (1) the presence of Ta–F bonds inside the material due to the NF_3 plasma in the super-cycle (about 9% F in the oxide from chemical analyses from XPS); (2) a slight shift in the maximum of intensity of the Ta4f7 and Ta4f5 peaks (Ta–O bonds). This seems to indicate that the Ta_2O_5 film obtained from the selective deposition process is not fully oxidized and may explain the small decrease in density as compared to PEALD Ta_2O_5.

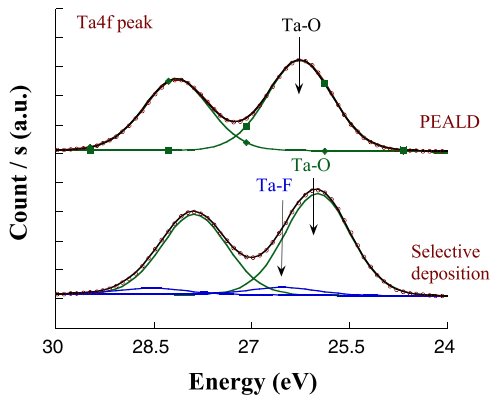

FIG. 11. (Color online) XPS spectra showing the Ta4f region of Ta_2O_5 films deposited on TiN substrate by PEALD or by selective deposition.

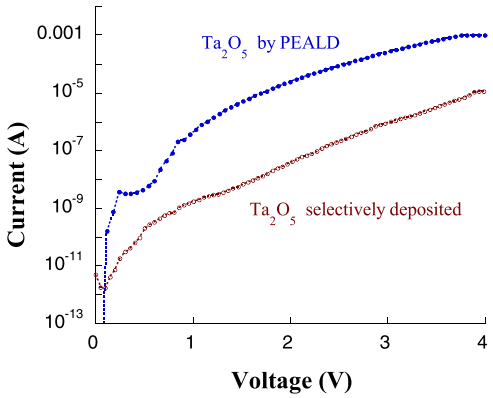

FIG. 12. (Color online) Leakage current of Ta_2O_5 MIM devices (Pt/Ta_2O_5 7 nm/TiN) vs voltage supply.

Nevertheless, Ta–F bonds may not be critical for the electrical properties of the oxide. Figure 12 shows the current–voltage (I-V) curve of metal insulator metal (MIM) devices made with 7 nm of Ta_2O_5. One is deposited by PEALD and the other one is deposited using the selective deposition process. The bottom electrode is TiN, and the top electrode is Pt deposited by evaporation. As can be observed in Fig. 12, better results are obtained using the selective deposition process with a leakage current that is 2 orders of magnitudes lower. This very first electrical result has to be confirmed in a future work, thanks to a statistical study on a high number of wafers.

IV. SUMMARY AND CONCLUSIONS

In this paper, we have demonstrated that we can selectively deposit Ta_2O_5 on TiN versus Si/SiO_2 by adding a plasma etching step to a PEALD process: 5 sccm of NF_3 is added to the O_2 plasma step every eight cycles in order to selectively remove the Ta_2O_5 layer from Si and SiO_2 versus TiN substrate. Si–F bonds at the surface also helps to increase the selective thickness by increasing the incubation time before starting the PEALD growth of Ta_2O_5 on Si or SiO_2 substrate. The presence of 9% F atoms in Ta_2O_5 layer is also found by XPS in the volume of the oxide in this first selective trial. The Fluor content does not seem to impact the electrical property of the deposited oxide. However, future work will be needed to evaluate possible effects on the Ta_2O_5 properties and decrease the Fluor content in the layers. This selective process has the advantage of being simple, easy to integrate, and compatible with standard microelectronics processing, with no use of SAMs, and seems not to be limited to Ta_2O_5 deposition. In particular, we will next focus on the results of selective deposition of TiO_2 on metallic surfaces versus insulators.

ACKNOWLEDGMENTS

This work was supported by the European project *PANACHE* and by the French Government program "Investissements d'Avenir" managed by the National Research Agency (ANR) under the Contract No. ANR-10-IQPX-33.

[1]K. Galatsis *et al.*, Adv. Mater. **22**, 769 (2010).
[2]D. C. Flanders and N. N. Efremow, J. Vac. Sci. Technol., B **1**, 1105 (1983).
[3]W. Shiu, H. Liu, J. Wu, T. Tseng, C. Te Liao, C. Liao, J. Liu, and T. Wang, Proc. SPIE **7274**, 72740E (2009).
[4]H. B. Profijt, S. E. Potts, M. C. M. van de Sanden, and W. M. M. Kessels, J. Vac. Sci. Technol., A **29**, 050801 (2011).
[5]S. Babin, G. Glushenko, T. Weber, T. Kaesebier, E.-B. Kley, and A. Szeghalmi, J. Vac. Sci. Technol., B **30**, 031605 (2012).
[6]M. Yan, Y. Koide, J. R. Babcock, P. R. Markworth, J. A. Belot, T. J. Marks, and R. P. H. Chang, Appl. Phys. Lett. **79**, 1709 (2001).
[7]M. H. Park, Y. J. Jang, H. M. Sung-Suh, and M. M. Sung, Langmuir **20**, 2257 (2004).
[8]R. Chen, H. Kim, P. C. McIntyre, and S. F. Bent, Appl. Phys. Lett. **84**, 4017 (2004).
[9]R. Chen, H. Kim, P. C. McIntyre, D. W. Porter, and S. F. Bent, Appl. Phys. Lett. **86**, 191910 (2005).
[10]K. J. Park, J. M. Doubt, T. Gougousi, and G. N. Parsons, Appl. Phys. Lett. **86**, 051903 (2005).
[11]E. Färm, M. Kemell, M. Ritala, and M. Leskelä, Chem. Vap. Deposition **12**, 415 (2006).
[12]R. Chen, H. Kim, P. C. McIntyre, and S. F. Bent, Chem. Mater. **17**, 536 (2005).
[13]F. S. M. Hashemi, C. Prasittichai, and S. F. Bent, ACS Nano **9**, 8710 (2015).
[14]A. Sinha, D. W. Hess, and C. L. Henderson, J. Vac. Sci. Technol., B **24**, 2523 (2006).
[15]H. B. R. Lee and S. F. Bent, *Atomic Layer Deposition of Nanostructured Materials*, edited by. N. Pinna and M. Knez (Wiley, 2012).
[16]A. J. M. Mackus, A. A. Bol, and W. M. M. Kessels, Nanoscale **6**, 10941 (2014).
[17]X. Jiang and S. F. Bent, J. Electrochem. Soc. **154**, D648 (2007).
[18]E. Färm, M. Vehkamäki, M. Ritala, and M. Leskelä, Semicond. Sci. Technol. **27**, 074004 (2012).
[19]E. Färm, S. Lindroos, M. Ritala, and M. Leskelä, Chem. Mater. **24**, 275 (2012).
[20]H. B. R. Lee, M. N. Mullings, X. Jiang, B. M. Clemens, and S. F. Bent, Chem. Mater. **24**, 4051 (2012).
[21]W. Dong, K. Zhang, Y. Zhang, T. Wei, Y. Sun, X. Chen, and N. Dai, Sci. Rep. **4**, 4458 (2014).
[22]M. N. Mullings, H. B. R. Lee, N. Marchack, X. Jiang, Z. Chen, Y. Gorlin, K. P. Lin, and S. F. Bent, J. Electrochem. Soc. **157**, D600 (2010).
[23]G. Gay *et al.*, Nanotechnology **21**, 435301 (2010).
[24]M. Fang and J. C. Ho, ACS Nano **9**, 8651 (2015).
[25]M. Reinke, Y. Kuzminykh, and P. Hoffmann, ACS Appl. Mater. Interfaces **7**, 9736 (2015).
[26]R. H. A. Ras, E. Sahramo, J. Malm, J. Raula, and M. Karppinen, J. Am. Chem. Soc. **130**, 11252 (2008).
[27]P. R. Chalker, P. A. Marshall, K. Dawson, I. F. Brunell, C. J. Stucliffe, and R. J. Potter, AIP Adv. **5**, 017115 (2015).
[28]S. E. Atanasov, B. Kalanyan, and G. N. Parsons, J. Vac. Sci. Technol., A **34**, 01A148 (2016).
[29]K. J. Hughes and J. R. Engstrom, J. Vac. Sci. Technol., A **30**, 01A102 (2012).
[30]F. Piallat, C. Vallée, R. Gassilloud, P. Michallon, B. Pelissier, and P. Caubet, J. Phys. D: Appl. Phys. **47**, 185201 (2014).
[31]F. Piallat and J. Vitiello, J. Vac. Sci. Technol., B **34**, 021202 (2016).
[32]M. Aoukar, P. D. Szkutnik, D. Jourde, B. Pelissier, P. Michallon, P. Noé, and C. Vallée, J. Phys. D: Appl. Phys. **48**, 265203 (2015).
[33]S.-W. Choi, C.-M. Jang, D.-Y. Kim, J.-S. Ha, H.-S. Park, W. Koh, and C.-S. Lee, J. Korean Phys. Soc. **42**, S975 (2003).
[34]S. Seki, T. Unagami, and B. Tsujiyama, J. Electrochem. Soc. **130**, 2505 (1983).
[35]K. P. Lee, K. B. Jung, R. K. Singh, S. J. Pearton, C. Hobbs, and P. Tobin, J. Vac. Sci. Technol., A **18**, 1169 (2000).
[36]Y. Kuo, J. Electrochem. Soc. **139**, 579 (1992).
[37]E. Atanassova and D. Spassov, Appl. Surf. Sci. **135**, 71 (1998).